Supplemental Data

How the T Cell Repertoire Becomes

Peptide and MHC Specific

Eric S. Huseby, Janice White, Frances Crawford, Tibor Vass, Dean Becker, Clemencia Pinilla, Philippa Marrack, and John W. Kappler

Supplemental Experimental Procedures

Generation of Transgenic Mice Expressing IA^b + 3K-Specific TCR

Full-length rearranged TCR cDNAs for TCR α and β chains were cloned from the IA^b + 3K-specific hybridomas: YAe5 62.8 (Vα4.12 and Vβ8.2 TCR); 2W1S12 20.4 T cell (Vα2.9 and Vβ8.2 TCR) and 3K-36 (Vα3.4, Vβ8.2 TCR) using PCR primers corresponding to sequences 5' to the start and 3' of the stop of rearranged TCR chains. The primers used were
Vα2 – GCTTCAGTCTAGGAGGAATGG;
Vα3 – CACCATGCTCCTGGCACTCCTCCCA;
Vα4.12 – TTGCTGGGTCCGCGGTGACTCAGTGACCCAGATGCAAG;
Cα – TGAATGGTCAGCAGCAGTGAG;
Vβ8.2 – GGTCCCAAGATGGGCTCCAGGCTC; and
Cβ1 – GGATCCCTTCATGAATTTTTTCTTTTGACCATAGCC.
The PCR products were cloned into an EcoRI restriction site using the PCR2.1 T/A cloning kit (Stratagene). The variable regions of the B3K 506 T cell (Vα4.1 and Vβ8.1 TCR), B3K 508 T cell (Vα2.3, Vβ14 TCR), 75-55 (Vα4.11, Vβ8.2), 74-1 (Vβ14, Vα4.11), 75-1 (Vβ8.1, Vα2) were cloned by fusing the TCRα chains to the Cα region of the 20.4 TCRα chain by introducing a BspEI site 10 base pairs into the Cα region and a fusion of the TCR β chains to the 20.4 TCR β chain constant region via a Bgl2 site 2 base pairs into the Cβ region.
The PCR primers used were
Vα4.1 – GGGCTCGAGAAGATGGACTCTTCTCCAG;
Vα4.11– GTCCGCGGTGATTCAGTGACCCAGAAACAAGGTCAA
Vα2.3 – GGGCTCGAGAGGAATGGACACGATCCTGACAGCA;
Cα – CTGGTACACAGCAGGTTCCGGATTCTGGATGT;
Vβ8.1 – CCTGGGAACCAAACATATGGAGGCTGCAGTCA;
Vβ14 – CTGGGAACCAAACATATGGAGGCTCAGACTATCCATCAATG;
Cβ – CTTGGGTGGAGTCACATCTCTCAGATCTTC.

All the TCR genes were sequenced, and error-free cDNAs were subcloned into the human CD2 promoter transgene cassette for T cell–specific expression (Zhumabekov et al., 1995). All cloned TCRs were assessed for IA^b + 3K reactivity by transfection into a TCR deficient hybridoma. TCR Tg mouse lines were established by injecting C57BL/6 oocytes with the TCR Tg plasmids.

TCR/MHC Crystal-Structure Analysis

Ten TCR/MHC/peptide crystal structures were analyzed using the default settings of Protein Explorer (Martz, 2001) for electron donor/acceptor pairs (hydrogen bonds and salt bridges for pairs less then 3.5 angstroms apart) as well as for hydrophobic interactions less than 4.5 angstroms apart (pdb files 1D9K, 1J8H, 1FYT, 2CKB, 1MWA, 1AO7, 1MI5, 1LP9, 1NAM,

1OGA) (Buslepp et al., 2003; Garboczi et al., 1996; Garcia et al., 1998; Hennecke et al., 2000; Hennecke and Wiley, 2002; Kjer-Nielsen et al., 2003; Luz et al., 2002; Reinherz et al., 1999; Reiser et al., 2003; Stewart-Jones et al., 2003). Backbone interaction were characterized to include atoms of the peptide bond as well as the amino acid α and β (except for Gly) carbons.

Supplemental References

Buslepp, J., Wang, H., Biddison, W. E., Appella, E., and Collins, E. J. (2003). A correlation between TCR Valpha docking on MHC and CD8 dependence: implications for T cell selection. Immunity *19*, 595-606.

Endres, R. O., Marrack, P., and Kappler, J. W. (1983). An IL 2-secreting T cell hybridoma that responds to a self class I histocompatibility antigen in the H-2D region. J Immunol *131*, 1656-1662.

Garboczi, D. N., Ghosh, P., Utz, U., Fan, Q. R., Biddison, W. E., and Wiley, D. C. (1996). Structure of the complex between human T-cell receptor, viral peptide and HLA-A2. Nature *384*, 134-141.

Garcia, K. C., Degano, M., Pease, L. R., Huang, M., Peterson, P. A., Teyton, L., and Wilson, I. A. (1998). Structural basis of plasticity in T cell receptor recognition of a self peptide-MHC antigen. Science *279*, 1166-1172.

Hennecke, J., Carfi, A., and Wiley, D. C. (2000). Structure of a covalently stabilized complex of a human alphabeta T-cell receptor, influenza HA peptide and MHC class II molecule, HLA-DR1. Embo J *19*, 5611-5624.

Hennecke, J., and Wiley, D. C. (2002). Structure of a complex of the human alpha/beta T cell receptor (TCR) HA1.7, influenza hemagglutinin peptide, and major histocompatibility complex class II molecule, HLA-DR4 (DRA*0101 and DRB1*0401): insight into TCR cross-restriction and alloreactivity. J Exp Med *195*, 571-581.

Kjer-Nielsen, L., Clements, C. S., Purcell, A. W., Brooks, A. G., Whisstock, J. C., Burrows, S. R., McCluskey, J., and Rossjohn, J. (2003). A structural basis for the selection of dominant alphabeta T cell receptors in antiviral immunity. Immunity *18*, 53-64.

Liu, C. P., Crawford, F., Marrack, P., and Kappler, J. (1998). T cell positive selection by a high density, low affinity ligand. Proc Natl Acad Sci U S A *95*, 4522-4526.

Liu, X., Dai, S., Crawford, F., Fruge, R., Marrack, P., and Kappler, J. (2002). Alternate interactions define the binding of peptides to the MHC molecule IA(b). Proc Natl Acad Sci U S A *99*, 8820-8825.

Luz, J. G., Huang, M., Garcia, K. C., Rudolph, M. G., Apostolopoulos, V., Teyton, L., and Wilson, I. A. (2002). Structural comparison of allogeneic and syngeneic T cell receptor-peptide-major histocompatibility complex complexes: a buried alloreactive mutation subtly alters peptide presentation substantially increasing V(beta) Interactions. J Exp Med *195*, 1175-1186.

Martz, E. (2001). Protein Explorer Software. (http://proteinexplorerorg).

Pinilla, C., Appel, J. R., Blanc, P., and Houghten, R. A. (1992). Rapid identification of high affinity peptide ligands using positional scanning synthetic peptide combinatorial libraries. Biotechniques *13*, 901-905.

Reinherz, E. L., Tan, K., Tang, L., Kern, P., Liu, J., Xiong, Y., Hussey, R. E., Smolyar, A., Hare, B., Zhang, R., *et al.* (1999). The crystal structure of a T cell receptor in complex with peptide and MHC class II. Science *286*, 1913-1921.

Reiser, J. B., Darnault, C., Gregoire, C., Mosser, T., Mazza, G., Kearney, A., van der Merwe, P. A., Fontecilla-Camps, J. C., Housset, D., and Malissen, B. (2003). CDR3 loop flexibility contributes to the degeneracy of TCR recognition. Nat Immunol *4*, 241-247.

Stewart-Jones, G. B., McMichael, A. J., Bell, J. I., Stuart, D. I., and Jones, E. Y. (2003). A structural basis for immunodominant human T cell receptor recognition. Nat Immunol *4*, 657-663.

Young, A. C., Zhang, W., Sacchettini, J. C., and Nathenson, S. G. (1994). The three-dimensional structure of H-2Db at 2.4 A resolution: implications for antigen-determinant selection. Cell *76*, 39-50.

Zhumabekov, T., Corbella, P., Tolaini, M., and Kioussis, D. (1995). Improved version of a human CD2 minigene based vector for T cell-specific expression in transgenic mice. J Immunol Methods *185*, 133-140.

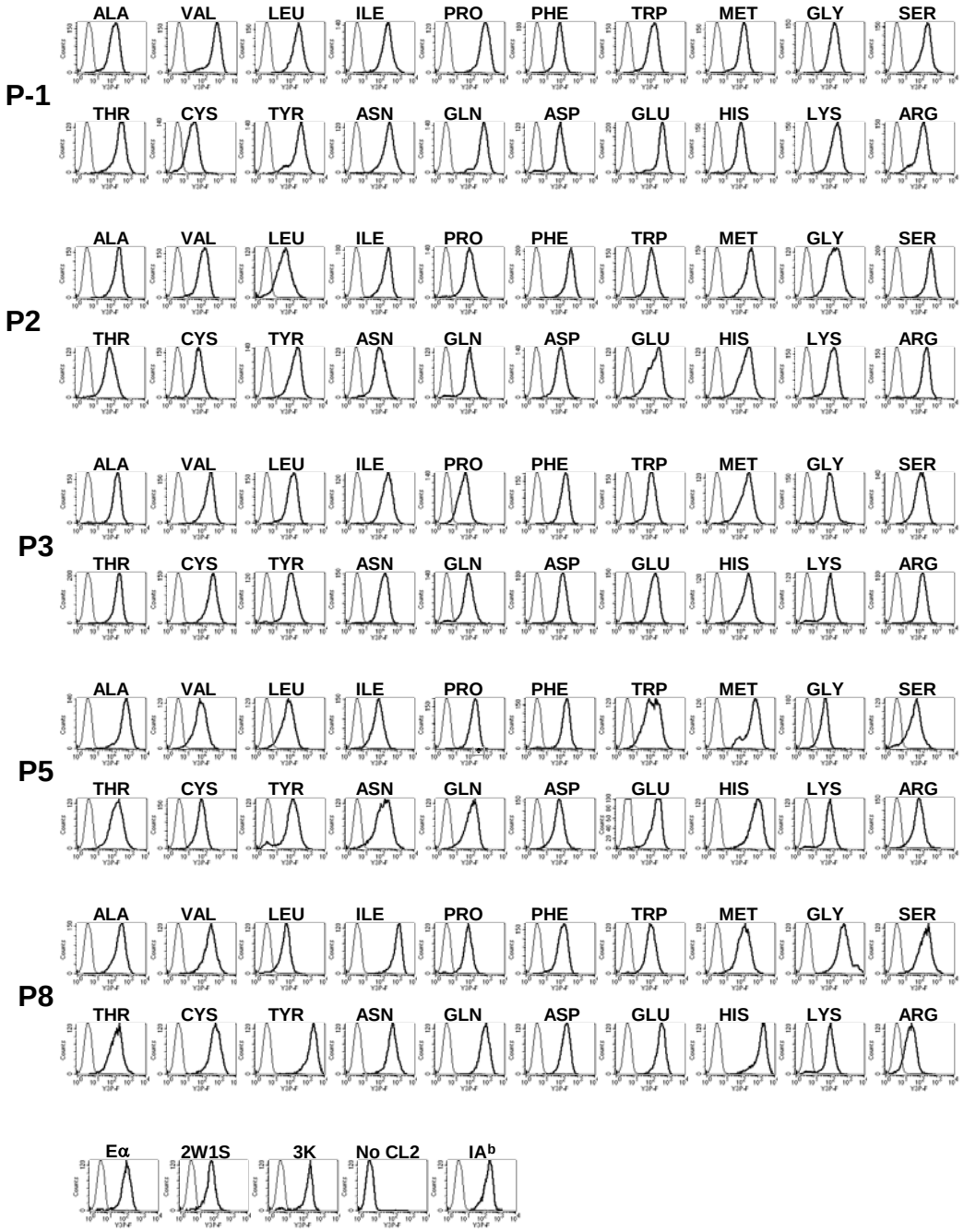

Figure S1. Expression of IA^b + 3K or Single-Amino Acid Substitutions at Each of the Five Potential TCR Contact Residues

IA^{b}bβ-/- Ii-/- C57BL/6 fibroblasts were transduced with retroviruses expressing the IAbα and peptide linked IA^{b}β proteins, cloned and selected for cells expressing similar levels of MHC class II as assessed by the staining with the anti-MHC Class II antibody Y3P.

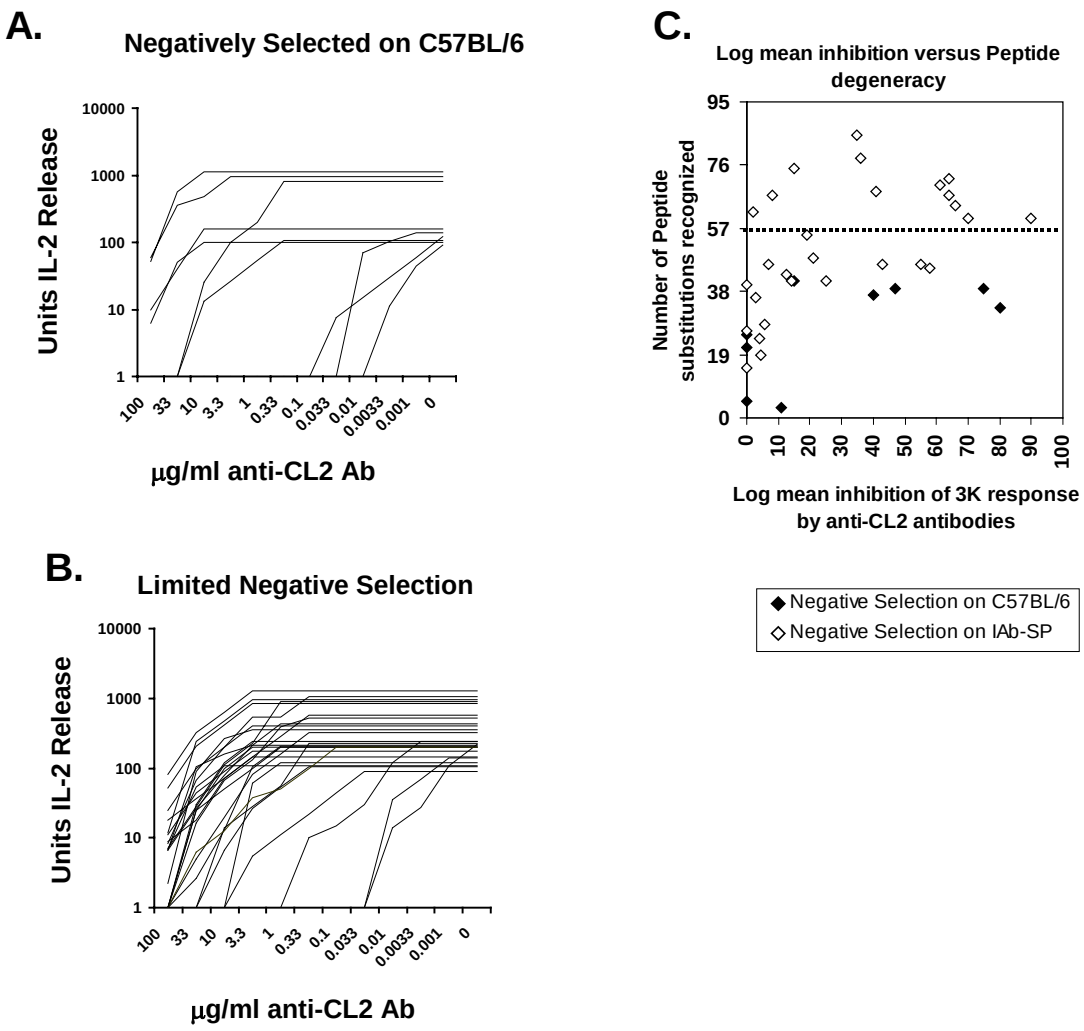

Figure S2. The T Cell Repertoires in Negative-Selection Sufficient and Limited Mice Contain a Range of TCR Affinities for the Immunizing IA^b + 3K Antigen

(A and B) Individual IAb + 3K specific T cell hybridomas isolated from (A) C57BL/6 or chimeric mice in which IAb-SP mice were reconstituted with C57BL/6 BM, or (B) IA^b-SP, IA^b-SP mice reconstituted with IA^bb-SP BM or CL2-/- mice, were activated with APC expressing IA^b + 3K in the presence of titrated amounts of a cocktail of anti-IAb monoclonal antibodies (M5/114, 3F12 and Y3P). Data were generated by averaging results from 2 independent experiments.

(C) The concentration of anti-IA^b monoclonal antibodies that inhibited the mean log of the response was calculated and plotted against the number of peptide substitutions recognized from Figure 2. T cells negatively selected on IA^b-SP (◊) have a range of affinity and peptide degeneracy, which overlaps that of T cells from mice negatively selected on wt IAb (♦). The dashed line indicates TCRs with degeneracy significantly ($p<0.05$) different then those of TCRs isolated from C57BL/6 mice. Specificity controls for the antibody inhibition experiments included the inability of the cocktail to inhibit the activation of a MHC class I restricted T cell hybridoma 3DT.52.5.24 (Endres et al., 1983).

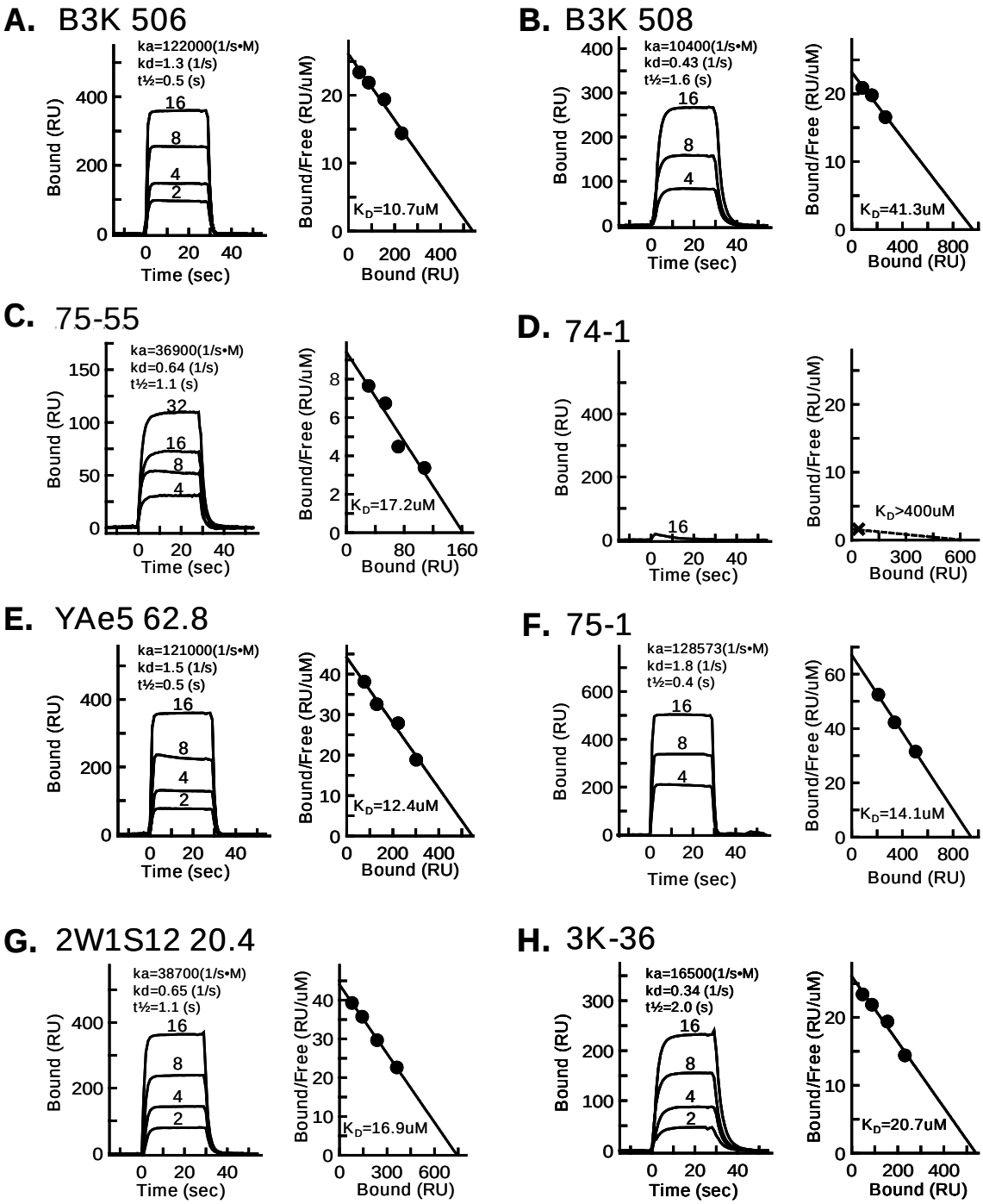

Figure S3. Kinetics and Scatchard Analysis of the Interaction of IA^b + 3K with Immobilized 3K-Specific TCRs

The affinity and kinetics of soluble, monomeric IA^b-3K binding to immobilized αβTCRs from IA^b-3K reactive T cell hybridomas was analyzed by surface plasmon resonance as previously described (Liu et al., 1998) using a BIAcore 2000 instrument (BIAcore AB, Uppsala, Sweden) .

Approximately 1000-2000 RU of soluble αβTCR was captured on the surface of a biosensor flowcell by an immobilized anti-Cα Mab, ADO-304 (Liu et al., 1998). Various concentrations (2, 4, 8, 16 and/or 32μM) of soluble IA^b-3K were injected at 10 μl/min for 30s through CM5 biosensor flow cells in which (A,B) C57BL/6, (C-G) IA^b-SP derived or (H) MHC CL2-/- derived TCRs have been immobilized and the binding kinetics recorded. As a control for bulk fluid phase refractive index the IA^b-3K preparation was also injected through a fourth flow cell with an immobilized irrelevant TCR Ani 2.3 specific for HLA-DR52c. All samples reached equilibrium binding within 10 sec. The complex was allowed to dissociate for 30 sec between injections. Raw data were corrected for the bulk signal from buffer and IA^b-3K by performing identical injections through a flow cell in which an irrelevant αβTCR was immobilized. The data were further corrected for the loss of captured αβTCR during the series of injections based on the observed dissociation rate (kd) of the αβTCR from the anti-Cα Mab (~ 4.5×10^{-4}/sec). The data were analyzed with BIAcore Bioeval software. Because the binding kinetics were so rapid, the equilibrium data were used to determine the dissociation constant (KD). The kinetic data were used to determine the dissociation rate and half life (t½) of the MHC/TCR complex and the association rate (ka) was calculated from the KD and kd (ka=kd/KD). No detectable binding was seen for the 74-1 TCR to IA^b + 3K. By assuming a maximum possible equilibrium signal of 25RU at a 16 μM injection and an Rmax of 500RU, the maximal K_D for (D) 74-1 was estimated at >400 μM (dashed line).

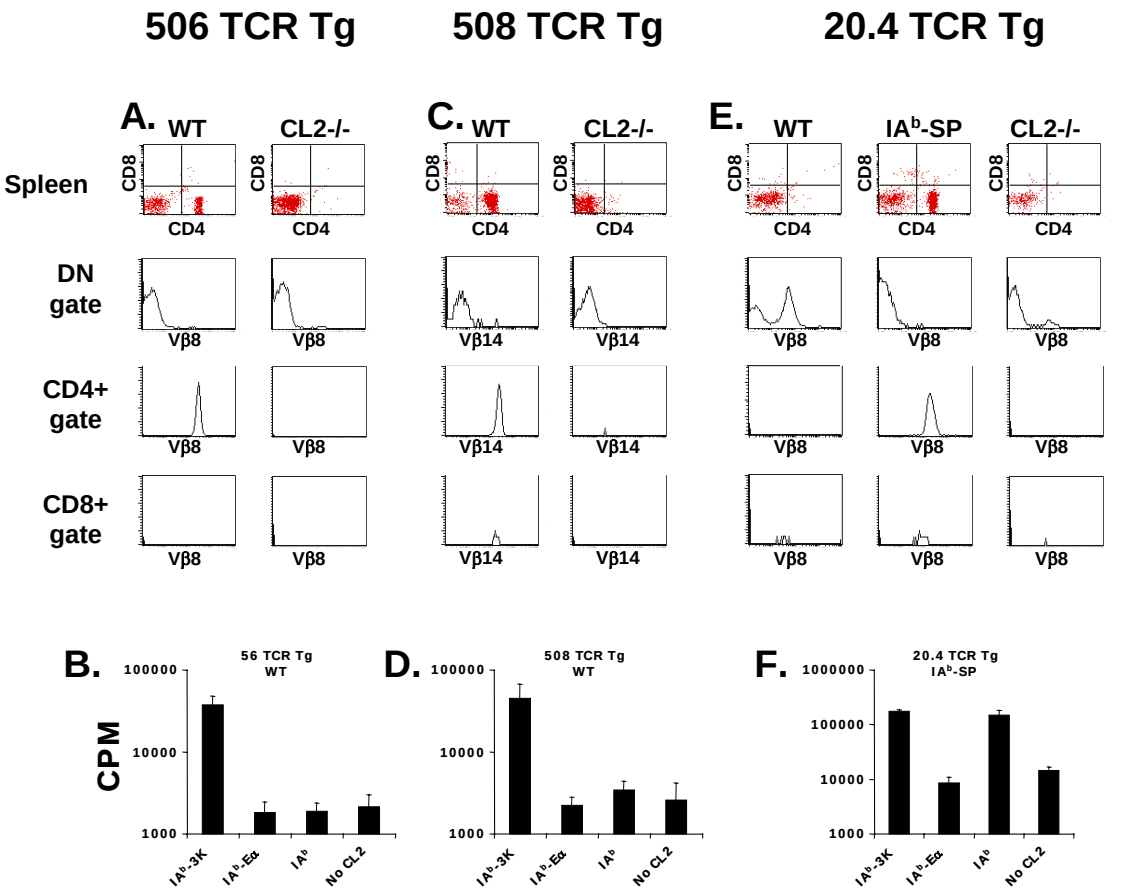

Figure S4. Rag1$^{-/-}$ Splenocytes Bearing Conventional IA^b + 3K-Specific TCRs Accumulate in the Spleen in an MHC Class II-Dependent Manner

Splenocytes were isolated from six week old mice and stained for expression of CD4 and CD8 and Vβ expressed by the relevant TCR. Each set of 4 vertical panels shows CD4 versus CD8 staining for splenocytes from the indicated TCR Tg on the indicated MHC background, followed by Vβ expression on the CD4-CD8- double negative or CD4$^+$ or CD8$^+$ T cells. (A) 506 and (C) 508 TCR Tg mice accumulate CD4$^+$ T cells in a class II-dependent manner which (B, D) proliferate in response to cells presenting IA^b + 3K. (E) DN T cells expressing the 20.4 TCR accumulate in the spleens of Rag1-/- mice with wild type IA^b, while CD4$^+$ T cells accumulate in spleens of IA^b-SP mice that (F) proliferate in response to cells expressing either IA^b + 3K or cells expressing wild type IA^b proteins. Very few T cells are present in 20.4 TCR Tg mice in the absence of IA^b.

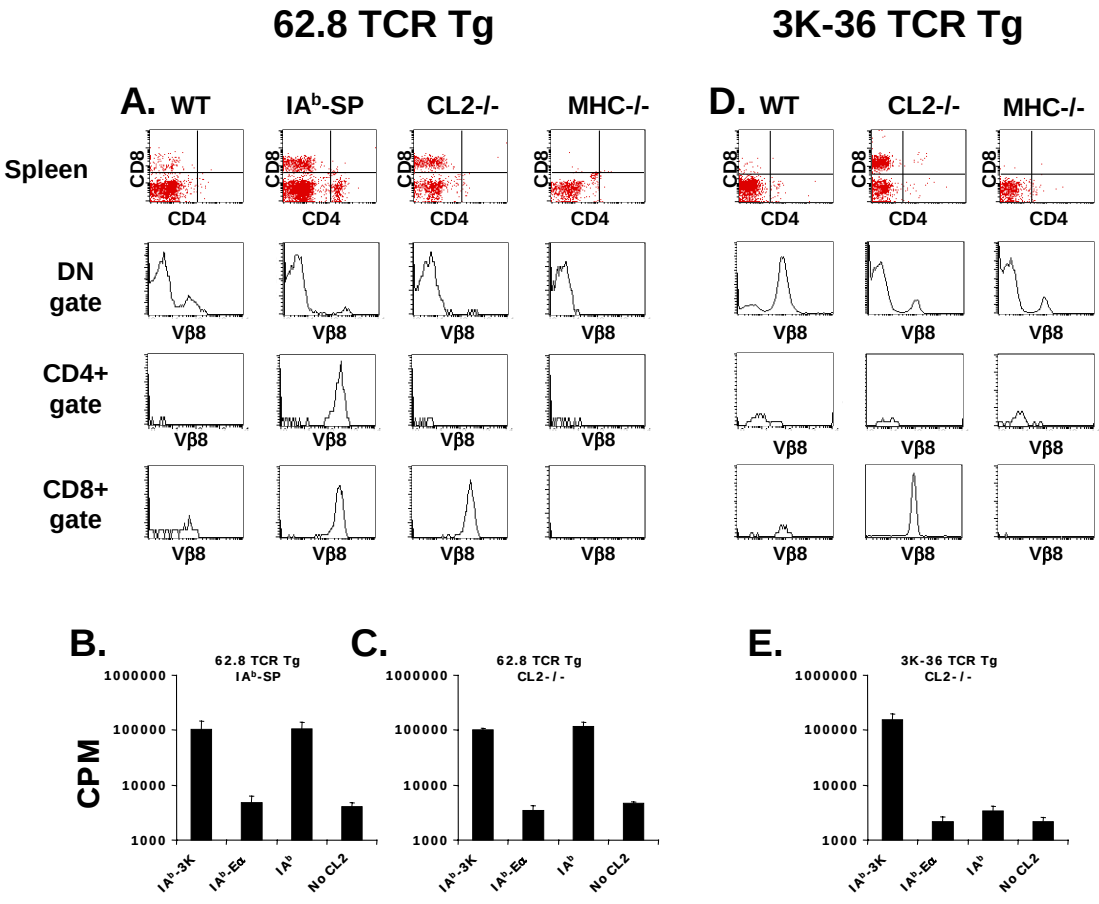

Figure S5. Rag1$^{-/-}$ Splenocytes Bearing Unconventional IA^b + 3K-Specific TCRs Accumulate in the Spleen in an MHC Class I or Class II-Dependent Manner

Splenocytes were isolated from six week old mice and stained for expression of CD4 and CD8 and Vβ expressed by the relevant TCR. Each set of 4 vertical panels shows CD4 versus CD8 staining for splenocytes from the indicated TCR Tg on the indicated MHC background, followed by Vβ expression on the CD4-CD8- double negative or CD4$^+$ or CD8$^+$ T cells.
(A) A minor population of DN and CD8$^+$ T cells accumulates in the spleen of 62.8 TCR Tg mice expressing wild type IA^b, while both CD4$^+$ and CD8$^+$ T cells accumulate in the spleens of mice expressing IA^b-SP. Only CD8$^+$ T cells accumulate in the spleen of 62.8 TCR Tg mice on an MHC CL2-/- background while no T cells are present in spleens of 62.8 MHC-/- mice.
(B and C) T cells from 62.8 TCR Tg mice on a (B) IA^b-SP background as well as on a (C) MHC CL2-/- background proliferate in response to APC presenting IA^b + 3K or wild type IA^b proteins.
(D) A large population of DN T cells accumulates in the spleens of 3K-36 TCR Tg mice on an MHC wild type background. CD8$^+$ T cells accumulate in the spleens of 3K-36 mice on an MHC CL2-/- background while T cells fail to accumulate in the spleens of MHC-/- mice.
(E) The CD8$^+$ T cells in MHC CL2-/- mice proliferate in response to APC expressing IA^b + 3K but not to wild type IA^b or control antigens.

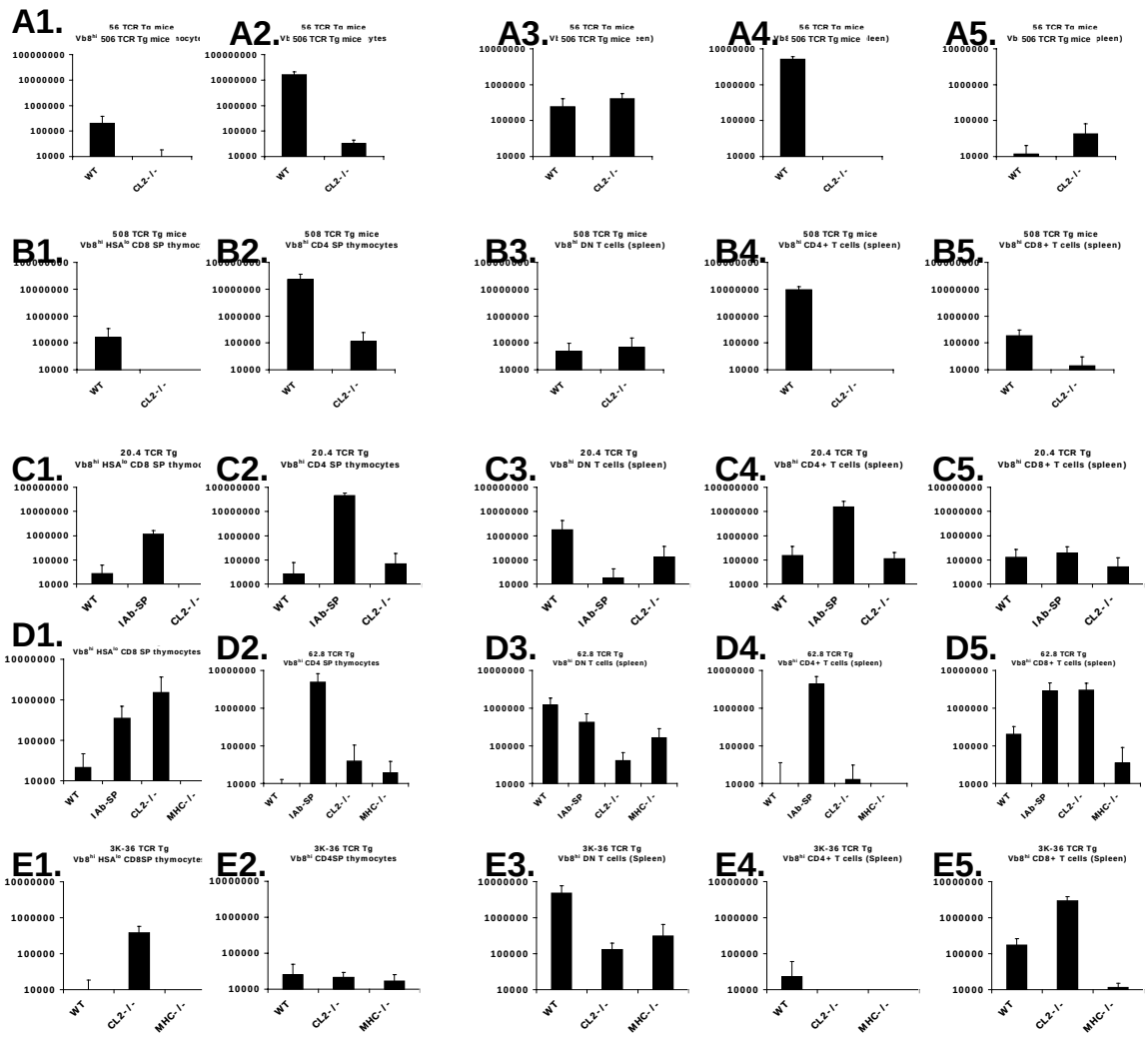

Figure S6. Thymic and Splenic Cell Counts of Rag1$^{-/-}$ (A1–A5) 506, (B1–B5) 508, (C1–C5) 20.4, (D1–D5) 62.8, and (E1–E5) 3K-36 TCR Tg Mice for Each of the Cell Populations Presented in This Study

Cell counts of (A1-E1) mature CD8$^+$ single positive Vβ high, HSA low thymocytes, and (A2-E2) mature CD4$^+$ single positive Vβ high thymocytes for Tg mice on each of the MHC backgrounds presented in this study. Cell counts of (A3-E3) CD4-CD8- double negative, Vβ high; (A4-E4) CD4$^+$, Vβ high and (A5-E5) CD8$^+$, Vβ high splenocytes for Tg mice on each of the MHC backgrounds presented. Data is compiled from at least 5 mice, 5-8 weeks old on each genetic background.

	100 ug/ml + B2M	33 ug/ml + B2M	10 ug/ml + B2M	100 ug/ml No B2M	33 ug/ml No B2M
AA	**P1**	**P1**	**P1**	**P1**	**P1**
K	12.5	1.6	1.1	2.6	1.8
V	14.2	1.2	0.6	2.0	1.2
W	13.3	1.2	1.1	2.2	1.8
A	3.2	1.4	1.0	2.3	1.6
S	3.7	1.5	0.9	2.2	1.6

	100 ug/ml + B2M	33 ug/ml + B2M	10 ug/ml + B2M	100 ug/ml No B2M	33 ug/ml No B2M
AA	**P2**	**P2**	**P2**	**P2**	**P2**
I	17.6	3.7	1.1	1.9	1.4
V	14.2	1.2	0.6	2.0	1.2
R	11.7	1.1	0.7	1.7	1.6
G	5.5	1.7	1.2	2.2	1.7
H	3.7	1.1	0.8	2.4	1.8

	100 ug/ml + B2M	33 ug/ml + B2M	10 ug/ml + B2M	100 ug/ml No B2M	33 ug/ml No B2M
AA	**P3**	**P3**	**P3**	**P3**	**P3**
K	33.3	1.3	1.4	2.7	1.8
R	17.7	1.1	0.6	1.6	1.7
W	6.2	1.6	1.1	2.0	1.8
H	6.7	1.0	0.7	1.8	1.3
V	4.8	1.6	1.1	1.9	1.5

	100 ug/ml + B2M	33 ug/ml + B2M	10 ug/ml + B2M	100 ug/ml No B2M	33 ug/ml No B2M
AA	**P4**	**P4**	**P4**	**P4**	**P4**
W	21.3	2.7	0.9	2.9	2.3
L	13.3	1.4	0.7	1.8	1.5
P	4.0	2.1	1.1	2.6	1.7
Y	9.2	1.7	1.0	2.4	1.6
H	5.0	1.8	1.0	2.2	1.9

	100 ug/ml + B2M	33 ug/ml + B2M	10 ug/ml + B2M	100 ug/ml No B2M	33 ug/ml No B2M
AA	**P5**	**P5**	**P5**	**P5**	**P5**
W	31.3	1.8	1.0	2.6	1.7
L	8.1	1.6	1.3	2.1	1.4
K	4.1	1.3	1.1	2.1	1.7
R	4.5	1.3	1.1	1.7	1.4
A	2.3	1.2	1.1	2.1	1.5

	100 ug/ml + B2M	33 ug/ml + B2M	10 ug/ml + B2M	100 ug/ml No B2M	33 ug/ml No B2M
AA	**P6**	**P6**	**P6**	**P6**	**P6**
R	11.8	1.3	0.9	4.1	1.7
H	8.0	1.7	1.1	1.9	1.7
F	3.3	1.4	1.0	1.7	1.6
W	2.7	1.3	0.9	1.7	1.6
Y	3.3	0.8	0.8	1.6	0.9

	100 ug/ml + B2M	33 ug/ml + B2M	10 ug/ml + B2M	100 ug/ml No B2M	33 ug/ml No B2M
AA	**P7**	**P7**	**P7**	**P7**	**P7**
R	28.0	3.0	0.9	17.5	1.8
V	5.2	2.1	1.0	1.4	1.2
P	3.6	1.9	0.9	1.8	1.2
W	2.6	1.2	1.0	2.0	1.7
L	2.9	1.3	1.1	1.6	1.3

	100 ug/ml + B2M	33 ug/ml + B2M	10 ug/ml + B2M	100 ug/ml No B2M	33 ug/ml No B2M
AA	**P8**	**P8**	**P8**	**P8**	**P8**
L	13.0	1.7	1.1	1.3	1.6
P	6.9	2.3	1.2	2.1	1.4
M	5.0	1.1	1.0	1.4	1.2
V	4.0	1.4	0.9	1.3	1.4
I	3.5	1.6	0.9	1.1	1.5

	100 ug/ml + B2M	33 ug/ml + B2M	10 ug/ml + B2M	100 ug/ml No B2M	33 ug/ml No B2M
AA	**P9**	**P9**	**P9**	**P9**	**P9**
K	9.3	1.5	1.1	2.0	1.3
V	6.7	2.2	1.2	1.8	1.6
I	6.2	1.8	0.8	1.5	1.8
M	5.9	2.5	1.4	2.1	1.8
L	5.6	2.0	1.2	2.1	1.7

Figure S7. Discovery of Peptides that Bind to Class I and Stimulate 3K-36

CD8$^+$ 3K-36 TCR Tg spleen cells were incubated with MHC class II-deficient spleen cells pulsed with varying doses of the TPI 921 library (Pinilla et al., 1992) with or without the addition of exogenous β2-microglobulin. Responses were compared to control wells. Responses are converted into stimulation index (response/background) and ranked from highest response to lowest. Only the top five amino acid positions are shown. Data is representative of 3 independent experiments.

									Stimulation Index			
									Peptide Conc.			
P1	P2	P3	P4	P5	P6	P7	P8	P9	100	10	1	0.1
K	I	K	L	L	R	R	L	K	1	1	1	1
K	I	K	L	L	R	R	L	V	2	1	1	1
K	I	K	L	W	R	R	L	K	5	1	1	1
K	I	K	L	W	R	R	L	V	11	21	2	1
K	I	K	W	L	R	R	L	K	3	4	1	1
K	I	K	W	L	R	R	L	V	3	2	1	1
K	I	K	W	W	R	R	L	K	3	16	2	1
K	I	K	W	W	R	R	L	V	dead	22	1	1
K	R	K	L	L	R	R	L	K	1	1	1	1
K	R	K	L	L	R	R	L	V	1	1	1	1
K	R	K	L	W	R	R	L	K	7	1	1	1
K	R	K	L	W	R	R	L	V	16	20	1	1
K	R	K	W	L	R	R	L	K	4	2	1	1
K	R	K	W	L	R	R	L	V	4	1	1	1
K	R	K	W	W	R	R	L	K	15	3	1	1
K	R	K	W	W	R	R	L	V	12	20	1	1
V	I	K	L	L	R	R	L	K	2	1	1	1
V	I	K	L	L	R	R	L	V	3	1	1	1
V	I	K	L	W	R	R	L	K	4	2	1	1
V	I	K	L	W	R	R	L	V	17	15	1	1
V	I	K	W	L	R	R	L	K	3	5	1	1
V	I	K	W	L	R	R	L	V	10	5	1	1
V	I	K	W	W	R	R	L	K	5	17	3	1
V	I	K	W	W	R	R	L	V	2	22	5	1
V	R	K	L	L	R	R	L	K	1	1	1	1
V	R	K	L	L	R	R	L	V	20	2	1	1
V	R	K	L	W	R	R	L	K	16	1	1	1
V	R	K	L	W	R	R	L	V	14	13	1	1
V	R	K	W	L	R	R	L	K	5	2	1	1
V	R	K	W	L	R	R	L	V	20	1	1	1
V	R	K	W	W	R	R	L	K	14	8	1	1
V	R	K	W	W	R	R	L	V	5	12	1	1
W	I	K	L	L	R	R	L	K	1	1	1	1
W	I	K	L	L	R	R	L	V	1	1	1	1
W	I	K	L	W	R	R	L	K	1	1	1	1
W	I	K	L	W	R	R	L	V	1	18	2	1
W	I	K	W	L	R	R	L	K	dead	5	1	1
W	I	K	W	L	R	R	L	V	dead	2	1	1
W	I	K	W	W	R	R	L	K	dead	8	1	1
W	I	K	W	W	R	R	L	V	dead	21	1	1
W	R	K	L	L	R	R	L	K	2	1	1	1
W	R	K	L	L	R	R	L	V	1	1	1	1
W	R	K	L	W	R	R	L	K	2	1	1	1
W	R	K	L	W	R	R	L	V	8	8	1	1
W	R	K	W	L	R	R	L	K	4	2	1	1
W	R	K	W	L	R	R	L	V	dead	1	1	1
W	R	K	W	W	R	R	L	K	dead	4	1	1
W	R	K	W	W	R	R	L	V	dead	20	1	1
P	F	D	S	Q	E	G	R	Q	1	1	1	1

Figure S8. Confirmation of the Specificity of 3K-36 for Class I + Peptides

A series of peptides corresponding to the most active amino acid at each of the 9 positions as identified in Supplemental Figure 5 were synthesized and tested for the ability to activate the $CD8^+$ 3K-36 TCR Tg spleen cells. Responses have been converted into stimulation index (response/background). Data is representative of 3 independent experiments.

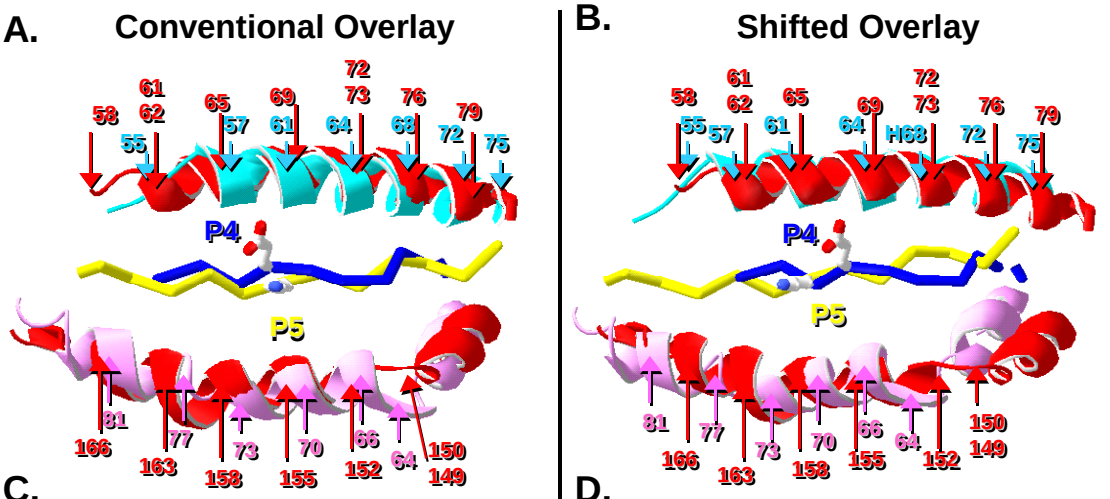

C.

Alpha	55	57	61	64	68	72	75
IA b, u	D	Q	Q	A	H	V	K
IA s	D	Q	Q	A	Y	I	K
IA f	D	Q	Q	A	H	I	K
IA q	D	Q	Q	A	H	G	K
IA d, g7, k	E	Q	Q	A	H	I	K
IE d, k	E	Q	A	A	A	V	E
IE u	E	Q	A	A	A	V	K

A1 domain	58	61	62	65	69	72	73	76	79
Kb	E	E	R	Q	G	Q	S	V	R
Kd	E	E	E	Q	S	Q	W	V	R
Kf	E	E	R	Q	S	Q	W	V	R
Kk	E	E	R	Q	G	Q	I	V	R
Db	E	E	R	Q	G	Q	W	V	R
Dd	E	E	R	R	G	Q	S	V	R
Dk	E	E	R	Q	G	Q	S	V	R
Dq	E	E	R	Q	D	Q	W	V	R
Dp	E	E	Q	Q	D	Q	S	V	R
Ld, q	E	E	R	Q	G	Q	W	V	R

D.

Alpha	55	57	61	64	68	72	75
IA b, u	D	Q	Q	A	H	V	K
IA s	D	Q	Q	A	Y	I	K
IA f	D	Q	Q	A	H	I	K
IA q	D	Q	Q	A	H	G	K
IA d, g7, k	E	Q	Q	A	H	I	K
IE d, k	E	Q	A	A	A	V	E
IE u	E	Q	A	A	A	V	K

A1 domain	58	61	62	65	69	72	73	76	79
Kb	E	E	R	Q	G	Q	S	V	R
Kd	E	E	E	Q	S	Q	W	V	R
Kf	E	E	R	Q	S	Q	W	V	R
Kk	E	E	R	Q	G	Q	I	V	R
Db	E	E	R	Q	G	Q	W	V	R
Dd	E	E	R	R	G	Q	S	V	R
Dk	E	E	R	Q	G	Q	S	V	R
Dq	E	E	R	Q	D	Q	W	V	R
Dp	E	E	Q	Q	D	Q	S	V	R
Ld, q	E	E	R	Q	G	Q	W	V	R

E.

Beta	81	77	73	70	66	64
IA b, d	H	T	A	R	E	Q
IA f, g7 k, q	H	T	A	R	67-Y	Q
IA s	H	T	A	Q	67-Y	Q
IA u	Y	T	A	R	67-Y	Q
IE b, k, s, u	H	T	A	Q	E	Q
IE d	H	T	A	D	E	Q

A2 domain	166	163	158	155	152	150	149
Kb	E	T	A	R	E	A	Q
Kd	E	E	A	Y	D	A	Q
Kf	E	E	A	R	A	A	Q
Kk	E	T	A	R	D	A	Q
Db	E	E	A	H	A	S	Q
Dd	E	E	A	R	A	A	Q
Dk	E	T	A	R	A	A	Q
Dq	E	E	A	H	A	G	Q
Dp	E	A	A	T	A	A	Q
Ld	E	E	A	Y	A	A	Q
Lq	E	E	A	H	A	A	Q

F.

Beta	81	77	73	70	66	64
IA b, d	H	T	A	R	E	Q
IA f, g7 k, q	H	T	A	R	67-Y	Q
IA s	H	T	A	Q	67-Y	Q
IA u	Y	T	A	R	67-Y	Q
IE b, k, s, u	H	T	A	Q	E	Q
IE d	H	T	A	D	E	Q

A2 domain	166	163	158	155	152	150	149
Kb	E	T	A	R	E	A	Q
Kd	E	E	A	Y	D	A	Q
Kf	E	E	A	R	A	A	Q
Kk	E	T	A	R	D	A	Q
Db	E	E	A	H	A	S	Q
Dd	E	E	A	R	A	A	Q
Dk	E	T	A	R	A	A	Q
Dq	E	E	A	H	A	G	Q
Dp	E	A	A	T	A	A	Q
Ld	E	E	A	Y	A	A	Q
Lq	E	E	A	H	A	A	Q

Figure S9. A Comparison of Amino Acids at Potential TCR Contact Residues between Mouse MHC Class I and Class II Proteins Reveals Extensive Homology

(A and B) A (A) conventional and (B) shifted overlay of IAb (Liu et al., 2002) and Db (Young et al., 1994) show extensive structural homology at potential TCR contact residues of the IAbα (cyan) and IAbβ chain (magenta) with the Db αI and αII domain (red) including the overlap of the peptide's central up residue of Db with IAb.

(C and E) A conventional overlay of MHC class I and MHC class II show extensive amino acid homology at potential TCR contact residues of the MHC Class II β chains and MHC Class I αII domains with limited homology between the MHC class II α chain and the MHC class I αI domains.
(D and F) A shifted overlay of MHC class I and MHC class II however, shows extensive amino acid homology at potential TCR contact residues of the MHC Class II α chains and MHC Class I αI domains with limited homology between the MHC class II β chain and the MHC class I αII domains. Two amino acids are listed for MHC class I positions where both side chains have significant accessibility to the TCR interface.

TCR / MHC Crystal Structure	Contacts	Alpha	Peptide	Beta	% of total Interations which are with the backbone of: MHC	Peptide
D10 TCR on IA^k	**Backbone / Total**	**7/15**	**5/16**	**11/29**	**30**	**8**
Reinherz et al. Science 1999 (1D9K.pdb)						
HA TCR on DR4	**Backbone / Total**	**9/20**	**7/15**	**8/20**	**31**	**13**
Henneck et al. JEM 2002 (1J8H.pdb)						
HA TCR on DR1	**Backbone / Total**	**9/18**	**9/17**	**4/13**	**27**	**19**
Hennecke et al. EMBO 2000 (1FYT.pdb)						

		Alpha 1 domain	Peptide	Alpha 2 domain	% of total Interations which are with the backbone of: MHC	Peptide
2C TCR on K^b	**Backbone / Total**	**2/10**	**1/4**	**5/10**	**29**	**3**
Garcia et al. Science 1998 (2CKB.pdb)						
2C TCR on K^{bm3}	**Backbone / Total**	**6/15**	**2/11**	**5/12**	**29**	**5**
Luz et al. JEM 2002 (1MWA.pdb)						
A6 TCR on HLA-A2	**Backbone / Total**	**6/15**	**7/23**	**6/17**	**22**	**13**
Garboczi et al. Nature 1996 (1AO7.pdb)						
TCR on HLA-B8	**Backbone / Total**	**11/32**	**7/13**	**8/17**	**31**	**11**
Kjer-Nielsen et al. Immunity 2003 (1MI5.pdb)						
D^b TCR on HLA-A2	**Backbone / Total**	**7/17**	**3/3**	**14/26**	**46**	**7**
Buslepp et al. Immunity 2003 (1LP9.pdb)						
BM3 TCR on K^b	**Backbone / Total**	**12/19**	**2/6**	**5/12**	**46**	**5**
Reiser et al. Nature Imm. 2003 (1NAM.pdb)						
TCR on HLA-A2	**Backbone / Total**	**7/12**	**8/14**	**12/21**	**40**	**17**
Stewart-Jones et al. Nature Imm. 2003 (1OGA.pdb)						

Figure S10. TCR/MHC/Peptide Structures Show Considerable Numbers of Interactions between the TCRs and the Backbone of MHC

Ten TCR/MHC/peptide crystal structures were analyzed using the default settings of Eric Martz's Protein Explorer for electron donor/acceptor pairs (hydrogen bonds and salt bridges for pairs less then 3.5 angstroms apart) as well as for hydrophobic interactions less than 4.5 angstroms apart (Martz, 2001). Backbone interaction were characterized to include atoms of the peptide bond as well as Cα as well as Cβ sites.